

## Cooling of the Thermosphere by Atomic Oxygen

RICHARD A. CRAIG AND JOHN C. GILLE

*Dept. of Meteorology, Florida State University, Tallahassee*

(Manuscript received 27 September 1968)

### ABSTRACT

A detailed numerical integration of the equation of radiative transfer over the 62  $\mu$  line of atomic oxygen is described. The results show that the cooling rate  $h$  in the lower thermosphere is appreciably lower than the value ( $h_B$ ) given by Bates' approximate expression, and may even be negative near the mesopause. For the CIRA atmosphere,  $h/h_B=0.02, 0.21$  and  $0.50$  at altitudes 100, 110 and 120 km, respectively, and reaches 0.88 above 200 km. In relating cooling rates to temperature changes, a calculation of  $c_p$  is performed which includes the effects of dissociation and accessibility of vibrational levels. The latter leads to an increase of the same order as the former.

### 1. Introduction

Bates (1951) surveyed the radiative processes that might be significant in the thermosphere and pointed out the possible importance of the 62  $\mu$  line of atomic oxygen. In the same paper, he gave an expression for the heat loss in an optically thin atmosphere. Although this simplified expression must give an overestimate at all altitudes and is not even approximately correct in an optically thick region, it has frequently been used in thermospheric models (for example, Lagos and Mahoney, 1967). The purpose of this paper is to present the results of a detailed numerical integration of the equation of radiative transfer for the CIRA 1965 model atmosphere, and to compare the computed heat loss with what would be obtained from the Bates formula.

The ground term of atomic oxygen is a  $^3P$  term with three levels,  $J=2, J=1$  and  $J=0$ , in order of increasing energy. The last two lie, respectively, 0.020 and 0.028 eV above the first. Because of the relative values of the Einstein coefficients and of the energy differences, only the 1-2 transition is energetically significant. This gives rise to the 62  $\mu$  line and is the only one considered in this paper.

### 2. Basic assumptions and numerical values

We have assumed a Boltzmann distribution at all altitudes, so that the number density  $N_J$  of  $O(^3P_J)$  is related to the number density  $N$  of  $O(^3P)$  by

$$\frac{N_J}{N} = \frac{\omega_J \exp(-E_J/k_B T)}{\sum \omega_J \exp(-E_J/k_B T)}, \tag{1}$$

where  $\omega_J$  is the statistical weight of the  $J$ th level ( $\omega_J=2J+1$ ),  $E_J$  the energy above the ground level,  $k_B$  is Boltzmann's constant and  $T$  the kinetic temperature. This assumption rests on the fact that the radiative

transitions are strongly forbidden and was justified numerically by Bates (1951). The value of  $N$  is very closely the same as the total number density of atomic oxygen.

We have also assumed in view of the low pressures and high temperatures involved that the line has a Doppler shape. In this case the monochromatic absorption coefficient per atom is

$$(b_{21})_\nu = \frac{\omega_1 A_{12} c^2 \exp(-\nu^2/\alpha_D^2)}{8\pi^3 \omega_2 \nu_0^2 \alpha_D}, \tag{2}$$

where  $A_{12}$  is the Einstein coefficient for spontaneous emission, for which we have used the value  $8.9 \times 10^{-5} \text{ sec}^{-1}$ ,  $c$  the speed of light,  $\nu$  the frequency measured from the line center  $\nu_0$ , and  $\alpha_D$  the Doppler width, the distance from the center of the line where the absorption coefficient has  $e^{-1}$  of its value at the line center.

The Doppler width is given by

$$\alpha_D = \frac{\nu_0}{c} \left( \frac{2k_B T}{m} \right)^{1/2}, \tag{3}$$

$m$  being the mass of the atom.

The equation of transfer, for a pencil of radiation with specific intensity  $I_\nu$  in a distance  $ds$ , can first of all be written as

$$dI_\nu = -N_2 (b_{21})_\nu I_\nu ds + N_1 (b_{12})_\nu I_\nu ds + N_1 (a_{12})_\nu ds, \tag{4}$$

where  $(b_{21})_\nu$ ,  $(b_{12})_\nu$ , and  $(a_{12})_\nu$  are proportional, respectively, to the Einstein coefficients for absorption, stimulated emission, and spontaneous emission. Thus, the first term on the right of (4) represents absorption, the second term stimulated emission, and the third term spontaneous emission.

To put this in a more familiar form for radiative transfer calculations, one can express  $N_1$  and  $N_2$  in

terms of  $N$  from (1), and also express  $(b_{12})_\nu$  and  $(a_{12})_\nu$  in terms of  $(b_{21})_\nu$  by the usual relations among the Einstein coefficients; thus,

$$(b_{12})_\nu = (\omega_2/\omega_1)(b_{21})_\nu, \quad (5)$$

$$(a_{12})_\nu = (\omega_2/\omega_1)(2h\nu^3/c^2)(b_{21})_\nu. \quad (6)$$

After these substitutions and some manipulation, the equation of transfer can be written as

$$dI_\nu/(k_\nu N ds) = -(I_\nu - B_\nu), \quad (7)$$

where  $B_\nu$  is the blackbody specific intensity and  $k_\nu$  is an "effective" absorption coefficient defined by

$$k_\nu = (b_{21})_\nu(N_2/N)[1 - \exp(-E_1/kT)]. \quad (8)$$

The value of  $k_\nu$  (hereafter called the absorption coefficient) depends on both frequency and temperature. It is convenient to express it in the form

$$k_\nu(T) = W(T) \exp(-\nu^2/\alpha_D^2), \quad (9)$$

where  $W(T)$ , a function of temperature only, can be obtained by substituting from (1) and (2) in (8). The value of  $W(T)$  is about  $3.5 \times 10^{-18} \text{ cm}^2 (\text{atom})^{-1}$  at 200K and about  $3.6 \times 10^{-19} \text{ cm}^2 (\text{atom})^{-1}$  at 1000K. The term in square brackets on the right side of (8), which represents the effect of stimulated emission, makes a significant contribution to this large variation. The value of  $\alpha_D$  is about  $7.4 \times 10^6 \text{ sec}^{-1}$  at 200K and about  $1.6 \times 10^7 \text{ sec}^{-1}$  at 1000K.

### 3. Numerical calculation of the heating rate

The heating rate  $h$  at a level  $Z$  in the atmosphere may be written

$$\begin{aligned} h(Z) = & 2\pi \int_{\Delta\nu} N(Z)k_\nu(Z) \\ & \times \left[ \{B_\nu^*(Z_L) - B_\nu(Z_L)\} E_2\{\tau_\nu(Z)\} \right. \\ & - \int_{Z_L}^Z E_2\{\tau_\nu(Z) - \tau_\nu(Z')\} \frac{dB_\nu(Z')}{dZ'} dZ' \\ & + \int_Z^{Z_U} E_2\{\tau_\nu(Z') - \tau_\nu(Z)\} \frac{dB_\nu(Z')}{dZ'} dZ' \\ & \left. - B_\nu(Z_U) E_2\{\tau_\nu(Z_U) - \tau_\nu(Z)\} \right] d\nu, \quad (10) \end{aligned}$$

in which  $Z_U$  and  $Z_L$  are upper and lower boundaries,  $E_2$  is the second exponential integral, and  $\tau_\nu$  the monochromatic optical separation, perhaps best termed the optical height, measured upward from  $Z_L$ , given by

$$\tau_\nu(Z) = \int_{Z_L}^Z k_\nu(Z') N(Z') dZ'. \quad (11)$$

$B_\nu^*(Z_L)$  represents the intensity illuminating  $Z_L$  from below, which may differ from the local blackbody intensity  $B_\nu(Z_L)$ .

#### a. Choice of boundary conditions

The level  $Z_L = 80 \text{ km}$  was chosen as the level below which there was very little atomic oxygen.  $B_\nu^*(Z_L)$  would originate at the surface if there were no atmospheric opacity at  $62 \mu$  below 80 km. However,  $62 \mu$  is in the most intense portion of the  $\text{H}_2\text{O}$  rotation band (Goody, 1964, Table 5.5), so that a small amount of water vapor will act as a black radiator. While the exact value to use will depend somewhat on the relative position of the oxygen and water vapor lines, it has seemed reasonable to take  $B_\nu^*$  corresponding to a stratospheric temperature, for which we use 216K. If a higher temperature is desired (if, say, the oxygen line fell very exactly on a water vapor line, and the radiation originated closer to the stratopause), it would only be necessary to increase the lower boundary term by the ratio of the increase of  $(B_\nu^* - B_\nu)$  ( $B_\nu$  corresponds to 183K) to correct the values in Section 5. This would make a noticeable difference only in the region immediately above 80 km.

The level  $Z_U$  was chosen as 230 km, and the effect of the small amount of atomic oxygen above that level has been neglected. The results at the top will thus overestimate the cooling by a small amount. This effect may be estimated by noting that addition of the 50 km from 180–230 km resulted in a decrease in heating rate by less than 2% above 130 km. The percentage change was higher below 130 km, but absolute changes were small and the patterns were very similar.

Since the expression for  $k_\nu$  cannot be written conveniently as the product of two functions, one of temperature alone and one of frequency alone, there is no simple scaling procedure available. [See Goody (1964, pp. 234–235) for a discussion of this point.] We have therefore computed  $h$  by dividing the line into a number of small frequency intervals, numerically integrating (10) for each of them, and summing.

#### b. Integrating over the line

Consider the frequency interval  $\nu_i$  to  $\nu_{i+1}$ , where  $i=1$  corresponds to the center of the line. Define the mean absorption coefficient in this interval by

$$k(\nu_i, \nu_{i+1}, T) = \frac{\int_{\nu_i}^{\nu_{i+1}} k_\nu d\nu}{\nu_{i+1} - \nu_i}. \quad (12)$$

Substituting from (9) we get

$$k(\nu_i, \nu_{i+1}, T) = W(T) \left[ \frac{f(x_{i+1}) - f(x_i)}{x_{i+1} - x_i} \right], \quad (13)$$

where  $x_i = \nu_i/\alpha_D$  and  $f(x) = \int_0^x \exp(-y^2) dy$ , which is proportional to the error integral. Care must be taken in the numerical evaluation of (13), since the numerator is a very small difference between two relatively large numbers when  $x$  is large. However, a convenient and rapidly converging series results if one expands  $f(x_i)$  in a Taylor series around  $f(x_{i+1})$ , or follows some similar procedure.

In practice, we compared results of three different schemes for the integration over the line:

- 1)  $\Delta\nu = 10^6$  Hz,  $i = 1, 2, \dots, 20$  (on each side of the line center)
- 2)  $\Delta\nu = 10^6$  Hz,  $i = 1, 2, \dots, 30$  (on each side of the line center)
- 3)  $\Delta\nu = 0.75 \times 10^6$  Hz,  $i = 1, 2, \dots, 40$  (on each side of the line center)

The final results were not significantly different in the three cases; the results to be quoted below were based on 2). At 200K this scheme corresponds to an integration from the line center to about  $4\alpha_D$  with intervals of about  $0.13\alpha_D$ ; at 1000K these values, expressed in terms of  $\alpha_D$ , are about halved.

*c. Integration over the atmosphere*

The absorption coefficient  $k_i$  was calculated in the  $i$ th frequency interval at each kilometer from 80–230 km from the temperature at that level. The optical separations  $\Delta\tau_i(Z, Z+1)$  between two adjacent levels were obtained by integrating a cubic through values of  $k(Z)N(Z)$ . Summing  $\Delta\tau_i$  yields  $\tau_i(Z)$ . Values of  $\tau_i(Z)$ , of course, vary strongly with position from the line center. The variations of  $\tau$  with altitude are shown in

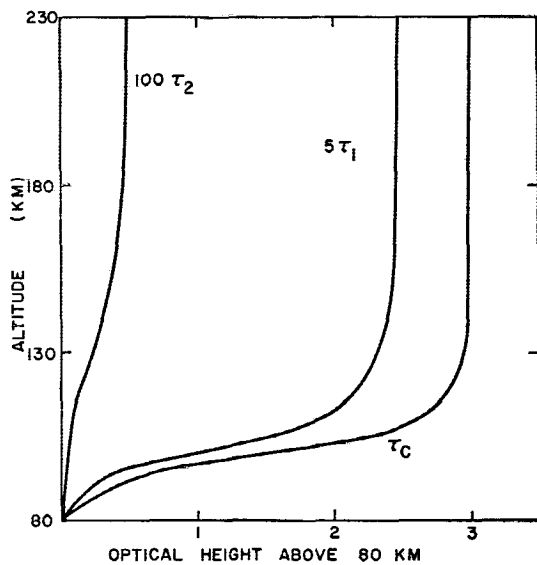


FIG. 1. Optical height measured upward from 80 km in three spectral intervals at the following distances from the line center (in units of  $10^6$  Hz):  $\tau_c$ , 0–1;  $\tau_1$ , 10–11;  $\tau_2$ , 20–21.

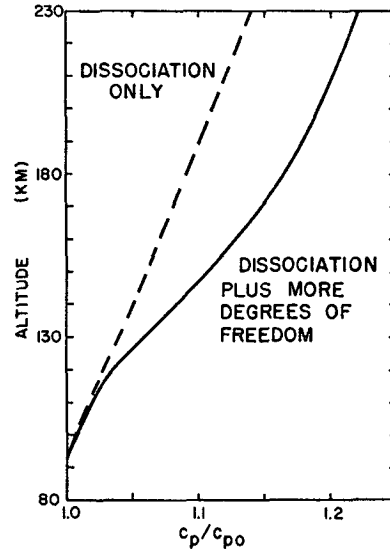


FIG. 2. Ratio of thermospheric specific heat to surface value, as a function of altitude. The dashed line indicates the result of considering only the dissociation of the diatomic species (Harris and Priester, 1962); the solid line includes the effect of temperature on the accessibility of the vibrational levels.

Fig. 1 for a spectral interval at the line center and two in the wings. At the top, the change of opacity per kilometer is very small, indicating that we have included all but a small fraction of the radiating atmosphere. The variation of the blackbody function over the line was neglected, and  $dB_\nu/dZ$  was obtained as  $(dB_\nu/dT)(dT/dZ)$ . The CIRA atmosphere contains first-order temperature discontinuities, so it was necessary to smooth the temperatures. This was done by first subtracting the linear trend and then expanding the remainder in a Fourier series. The atmospheric terms in (10) were evaluated with the trapezoidal rule.

**4. Computation of specific heats**

Under the assumption that the time rate of change of pressure is negligible, the temperature change due to heating may be written

$$\frac{dT}{dt} = \frac{h}{\rho c_p}, \tag{14}$$

where  $\rho$  is density and  $c_p$  the specific heat at constant pressure. For a single species,

$$\rho c_p = Ng(T)k_B,$$

in which  $g(T)$  is one plus half the number of effective degrees of freedom of the constituent. For an atomic constituent,  $g = \frac{5}{2}$ ; for a polyatomic molecule  $g(T)$  is an increasing function of temperature, since more excited states are accessible at higher temperatures, and thus more degrees of freedom are active. (Sears, 1953, p. 298 ff). In molecular oxygen and nitrogen, the transla-

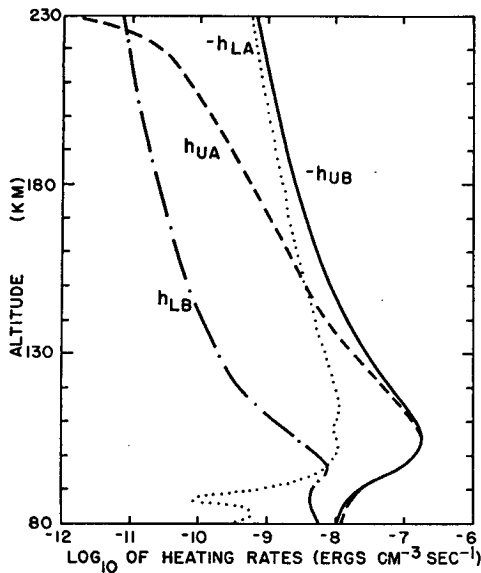


FIG. 3. Logarithmic plot of heating rates due to transfer in the  $62 \mu$  oxygen line, as functions of altitude. Solid line ( $-h_{UB}$ ), cooling to the upper boundary (space); dashed line ( $h_{UA}$ ), heating due to exchange with the overlying atmosphere; dotted line ( $-h_{LA}$ ), cooling to the underlying atmosphere; chain line ( $h_{LB}$ ), warming by radiation incident on the lower boundary from below.

tional and rotational degrees of freedom are excited at room temperature, but as the temperature is increased the vibrational degrees also become active. For a mixture of  $j$  species one has

$$\rho c_p = k_B \sum_j N_j g_j(T). \tag{15}$$

Using the tabulated constituents of the CIRA atmosphere and the  $g$  values of Hilsenrath *et al.* (1960),  $\rho c_p$  was calculated as a function of height. Values of  $c_p$

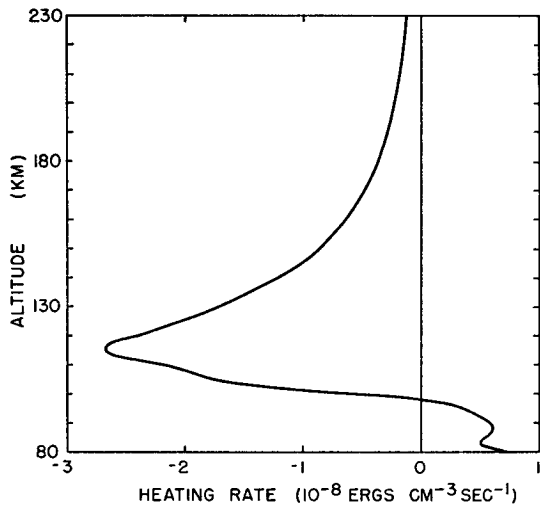


FIG. 4. Net heating rate  $h$  due to the atomic oxygen  $62 \mu$  line, as a function of altitude. Positive values show region of heating below 98 km.

increase with altitude because of the increasing degree of dissociation of the molecular species as well as the increase in  $g$ . The first effect, the only one considered by Harris and Priester (1962), is larger, but the two effects are usually comparable as shown in Fig. 2.

5. Computed heating rates

The terms in (1) may be designated  $h_{LB}$ ,  $h_{LA}$ ,  $h_{UA}$  and  $h_{UB}$  for the contribution by the lower boundary, underlying atmosphere, overlying atmosphere and upper boundary, respectively. Their variations with height are plotted in Fig. 3, and the variation of their sum is shown in Fig. 4. It will immediately be noticed that the warm overlying atmosphere and the lower boundary discontinuity lead to a net warming to almost 100 km. The cooling to space is always larger than loss

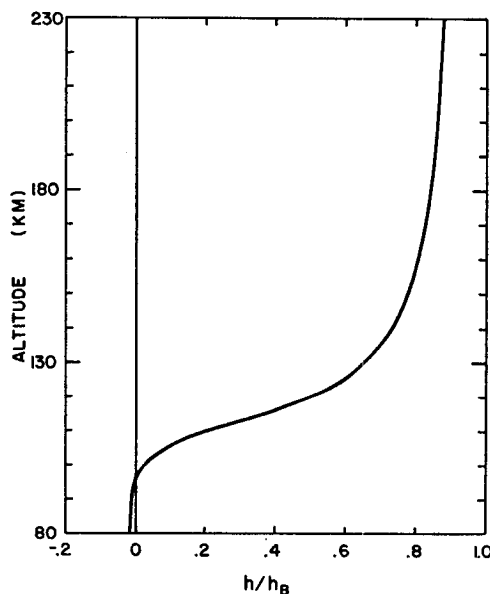


FIG. 5. Ratio of numerically calculated heating rate  $h$  to  $h_B$  given by Bates' (1951) approximation [Eq. (16)], as a function of altitude.

to the cooler region below, although the two are comparable at the highest altitudes. The net cooling reaches a maximum at 116 km.

It is most interesting to compare the numerical results with Bates' (1951) expression for an optically thin atmosphere, which may be written (Craig, 1965 p. 308) for  $h$  [erg cm<sup>-3</sup> sec<sup>-1</sup>] as

$$h_B = \frac{-1.67 \times 10^{-18} N \exp(-228/T)}{1 + 0.6 \exp(-228/T) + 0.2 \exp(-325/T)}. \tag{16}$$

The ratio  $h/h_B$  is plotted as a function of height in Fig. 5, which shows that, in addition to the heating to 98 km, exchange with the surrounding atmosphere and boundaries appreciably reduces cooling up to 130 km.

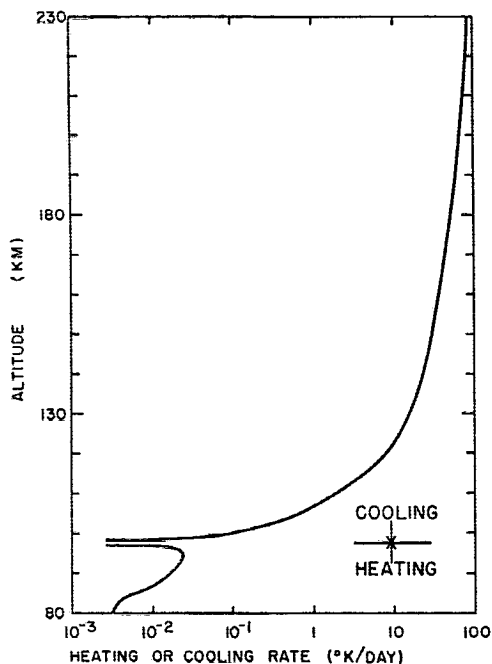


FIG. 6. Rate of change of temperature due to transfer in the  $62\text{-}\mu$  line plotted logarithmically as a function of altitude.

Because the lower layers have temperatures above absolute zero, energy is received from them and the cooling, even at the top of the layer considered, is only  $0.88 h_B$ .

The rate of change of temperature, calculated from (14) is shown in Fig. 6. This indicates that the heating below 100 km causes a temperature change less than  $3 \times 10^{-2} \text{K day}^{-1}$ , while the cooling leads to negative

rates of temperature change increasing monotonically to the top.

## 6. Conclusions

The results of numerically calculating the cooling due to transfer in the  $62\text{-}\mu$  oxygen line show that in the region 80–230 km Bates approximate expression overestimates the cooling, with errors over 50% below 130 km. Below 100 km there is a region of radiative warming, previously unnoticed, but the temperature change produced is very small.

*Acknowledgments.* This work was started while the authors were visiting scientists at the National Center for Atmospheric Research in the summer of 1967. Additional work was supported by the Atmospheric Sciences Section, National Science Foundation, under Grant GA-925.

## REFERENCES

- Bates, D. R., 1951: The temperature of the upper atmosphere. *Proc. Phys. Soc.*, **B64**, 805–821.
- Craig, R. A., 1965: *The Upper Atmosphere, Meteorology and Physics*. New York and London, Academic Press, 509 pp.
- Goody, R. M., 1964: *Atmospheric Radiation. I. Theoretical Basis*. Oxford, Clarendon Press, 436 pp.
- Harris, I., and W. Priestler, 1962: Time-dependent structure of the upper atmosphere. *J. Atmos. Sci.*, **19**, 286–301.
- Hilsenrath, J., et al., 1960: *Tables of Thermodynamic and Transport Properties*. New York, Pergamon Press, 478 pp.
- Lagos, C. P., and J. R. Mahoney, 1967: Numerical studies of seasonal and latitudinal variability in a model thermosphere. *J. Atmos. Sci.*, **24**, 88–94.
- Sears, F. W., 1953: *An Introduction to Thermodynamics, the Kinetic Theory of Gases, and Statistical Mechanics*. Reading, Pa., Addison-Wesley, 374 pp.